

Topological Mid-gap States of $p_x + ip_y$ Topological Superconductor with Vortex superlattice

Jiang Zhou,¹ Shi-Zhu Wang,¹ Ya-Jie Wu,¹ Rong-Wu Li,¹ and Su-Peng Kou^{1,*}

¹*Department of Physics, Beijing Normal University, Beijing 100875, PR China*

In this paper, the $p_x + ip_y$ topological superconductor with vortex superlattice is studied. We found that there exist mid-gap energy bands induced by the vortex superlattice and the mid-gap energy bands have nontrivial topological properties including the gapless edge states and non-zero winding number. An topological anisotropic tight-binding Majorana lattice model is proposed to describe the mid-gap states.

I. INTRODUCTION

The topological ordered states become active research fields in condensed matter physics[1, 2]. The first example is integer quantum Hall effect, of which people introduce a topological invariant (TKNN number) to describe the topological properties[3]. Recently, the topological insulators with Z2 topological invariant are proposed and realized in experiments[4, 5]. Another class of topological quantum states is the topological superconductor, of which an example is two dimensional $p_x + ip_y$ topological superconductor[6]. The $p_x + ip_y$ superconductor (SC) has full bulk gap and topologically protected Majorana edge states. In particular, for the two dimensional $p_x + ip_y$ topological superconductor, the quantized vortex traps Majorana fermion inside the vortex-core. So, there are 2^N -fold degenerate ground states for $2N$ vortices. The adiabatic exchanges of two vortices generate a unitary transformations in the 2^N dimensional Hilbert space, which implies the non-Abelian statistics for the vortices[7]. These Majorana zero modes trapped by the vortex-cores immune to any small perturbations, and thus are proposed to do topological quantum computation[8–11].

Recently, many theoretical and experimental efforts have been paid to the detection of

*Corresponding author; Electronic address: spkou@bnu.edu.cn

Majorana zero modes for the potential application [12, 13]. For the $p_x + ip_y$ SC, a single vortex associates a rigorous Majorana zero energy bound state. However, when taking two vortices nearby, the inter-vortex tunneling occurs and leads to a small energy splitting which removes the ground state degeneracy. Once the vortex is arranged regularly forming vortex lattice with vortex superlattice constant being the order of superconducting coherent length, the inter-vortex tunneling will modify the low energy band of $p_x + ip_y$ SC and induce mid-gap states.

In this paper, we focus on the $p_x + ip_y$ SC with vortex superlattice, of which the lattice constant is about $l \sim 2\xi$, where the coherent length can be estimated as the radius of profile of the wave function around the vortex. Our goal is to learn the nature of the mid-gap states induced by the vortex superlattice, then we use free Majorana lattice model to capture its properties. The paper is organized as follows. In Sec. II, we review the spinless $(p_x + ip_y)$ SC and show that a Majorana fermion with zero energy is trapped in the vortex core. In Sec. III, we present that the inter-vortex tunneling leads to the energy splitting and show the band structure of the mid-gap states of $p_x + ip_y$ SC with vortex superlattice. We also suggest a topological anisotropic Majorana lattice model to capture the low energy properties of the mid-gap states in this section. Finally, we conclude our discussion in Sec. IV.

II. THE MODEL OF $p_x + ip_y$ SUPERCONDUCTOR

In this section, firstly we review the $p_x + ip_y$ SC. We write down a lattice Hamiltonian for spinless fermions. From the corresponding BCS mean field theory, there exist two distinct phases, the weak pairing SC and the strong pairing SC, which are distinguished topologically. Then, we analyze the Bogoliubov-de Gennes (BdG) equation in the continuum limit and show that the zero energy bound state (zero mode) is described by a exponentially localized wave function.

A. Two dimensional $p_x + ip_y$ superconductor

For the sake of completeness, we now review the basis formalism of the $p_x + ip_y$ SC. The simplest form exhibiting $p_x + ip_y$ superconductivity is encoded in the following lattice

Hamiltonian H , where

$$\begin{aligned}
H &= H_0 + H_1, \\
H_0 &= -t \sum_{\mathbf{r}} \sum_{v=\hat{x}, \hat{y}} (c_{\mathbf{r}+v}^\dagger c_{\mathbf{r}} + h.c.) - u \sum_{\mathbf{r}} c_{\mathbf{r}}^\dagger c_{\mathbf{r}}, \\
H_1 &= -\frac{1}{2} \hat{\Delta} \sum_{\mathbf{r}} \{ (c_{\mathbf{r}+\hat{y}} c_{\mathbf{r}} - c_{\mathbf{r}-\hat{y}} c_{\mathbf{r}}) \\
&\quad - i(c_{\mathbf{r}+\hat{x}} c_{\mathbf{r}} - c_{\mathbf{r}-\hat{x}} c_{\mathbf{r}}) \} + h.c.
\end{aligned}$$

where u is the chemical potential, $\hat{\Delta}$ is the electron pairing function and t is the hopping strength, respectively. In the following parts, we set t to be energy unit. The operator $c_{\mathbf{r}}^\dagger/c_{\mathbf{r}}$ creates/destroys an electron on lattice site \mathbf{r} and satisfies the anti-commutation statistics $\{c_{\mathbf{r}}, c_{\mathbf{r}'}^\dagger\} = \delta_{\mathbf{r}\mathbf{r}'}$.

In terms of Nambu spinor $\Psi_{\mathbf{k}}^\dagger = (c_{\mathbf{k}}^\dagger, c_{-\mathbf{k}})$, the mean field Hamiltonian takes the form of

$$H = \frac{1}{2} \int_{\mathbf{k}} d\mathbf{k} \Psi_{\mathbf{k}}^\dagger H(\mathbf{k}) \Psi_{\mathbf{k}} \quad (1)$$

via the Fourier transformation into momentum, and $H(\mathbf{k})$ is a $2 \otimes 2$ matrix that reads

$$H(\mathbf{k}) = \begin{pmatrix} \xi(\mathbf{k}) & \Delta^*(\mathbf{k}) \\ \Delta(\mathbf{k}) & -\xi(\mathbf{k}) \end{pmatrix} \quad (2)$$

where $\xi(\mathbf{k}) = -2t(\cos \mathbf{k}_x + \cos \mathbf{k}_y) - u$. The pairing $\Delta(\mathbf{k}) = \sin \mathbf{k}_x + i \sin \mathbf{k}_y$ exhibits the p -wave (spin-triplet) symmetry as $\Delta(\mathbf{k}) = -\Delta(-\mathbf{k})$. The Hamiltonian H can be diagonalized by the Bogoliubov transformation $\alpha_{\mathbf{k}} = u_{\mathbf{k}} c_{\mathbf{k}} - v_{\mathbf{k}} c_{-\mathbf{k}}^\dagger$ so that $\{\alpha_{\mathbf{k}}, \alpha_{\mathbf{k}'}^\dagger\} = \delta_{\mathbf{k}\mathbf{k}'}$. The \mathbf{k} -dependent coefficients $u_{\mathbf{k}}$ and $v_{\mathbf{k}}$ can be determined according to the requirement that the full Hamiltonian has the diagonal form

$$H = \sum_{\mathbf{k}} E(\mathbf{k}) \alpha_{\mathbf{k}}^\dagger \alpha_{\mathbf{k}} + E_g \quad (3)$$

and the quasiparticle operator $\alpha_{\mathbf{k}}$ satisfies the anti-commutation relation. The quasi-particle excitation spectrum is given by

$$E(\mathbf{k}) = \sqrt{\xi^2(\mathbf{k}) + |\Delta(\mathbf{k})|^2}. \quad (4)$$

The energy gap closes at $|u| = 4t$, which can be used to define a topological quantum phase transition. For $|u| < 4t$, the system is in the weak pairing phase (topologically nontrivial phase). For $|u| > 4t$, the system is in a strong pairing phase (topological trivial phase). The quantum critical point at $|u| = 4t$ marks the phase transition between the weak pairing phase and the strong pairing phase.

B. The Majorana zero modes around SC vortex

To demonstrate the fact that a vortex in $p_x + ip_y$ SC traps a Majorana zero mode, we consider the low energy limit and make the substitution $\xi(\mathbf{k}) \approx -u(\mathbf{r})$. For a spatially slowly varying $u(\mathbf{r})$, we consider a domain wall $u(\mathbf{r}) < 0$ for $\mathbf{r} > \mathbf{r}_0$ and $u(\mathbf{r}) > 0$ for $\mathbf{r} < \mathbf{r}_0$. Since the different regions are in distinct topological phases, one expects edge states at the interface. It's sufficient to start with the continuum form

$$H_{BCS} = \int d^2\mathbf{r} \{ -u(\mathbf{r})\psi^\dagger\psi + [\frac{\Delta}{2}\psi^\dagger(\partial_x + i\partial_y)\psi^\dagger + h.c.] \}. \quad (5)$$

The Bogliubov-de-Gennes (BdG) matrix corresponding to this equation reads (see details in appendix)

$$H_{BdG}(\mathbf{r}) = \begin{pmatrix} -u(\mathbf{r}) & \{\Delta(\mathbf{r}), \partial_{\mathbf{r}} + i\partial_{\theta}/r\} \\ -\{\Delta^*(\mathbf{r}), \partial_{\mathbf{r}} - i\partial_{\theta}/r\} & u(\mathbf{r}) \end{pmatrix}, \quad (6)$$

with anticommutator being defined as $\{a, b\} = [ab + ba]/2$. To find the wave functions of the zero modes satisfying $H_{BdG}(\mathbf{r})\chi(\mathbf{r}) = E\chi(\mathbf{r})$, it's helpful to assume $\Delta(\mathbf{r}) = \Delta e^{-il\theta}$, which denotes the pairing with vorticity l located at position \mathbf{r} .

We solve the problem with the ansatz

$$\chi(\mathbf{r}) = \begin{pmatrix} e^{-i\theta/2}[f(r) + ig(r)] \\ e^{i\theta/2}[f(r) - ig(r)] \end{pmatrix} \quad (7)$$

where $f(r)$ and $g(r)$ obey

$$\begin{aligned} -iu(r)g - i\Delta\partial_r g - i\frac{\Delta(l-1)g}{2r} &= Ef, \\ u(r)f - \Delta\partial_r f - \frac{\Delta(l-1)f}{2r} &= Eg. \end{aligned} \quad (8)$$

Then, we find two zero modes located the boundary of the domain wall if $l = 1$. The wave functions of the zero modes are given by

$$\chi(\mathbf{r}) \sim e^{-\frac{1}{2}\int_{\mathbf{r}_0}^{\mathbf{r}} d\mathbf{r}' u(\mathbf{r}')} \begin{pmatrix} e^{-i\theta/2} \\ e^{i\theta/2} \end{pmatrix}. \quad (9)$$

The exponentially localized wave function corresponds to Majorana fermions due to the particle-hole symmetry.

To summarize, we have obtained the Majorana bound state (BS) with zero energy attached to a single $p + ip$ superconducting vortex. For the multi-vortex case, we need to take into account the inter-vortex tunneling.

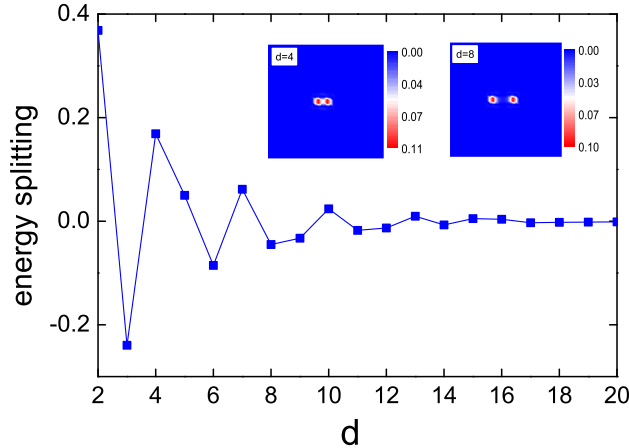


FIG. 1: (Color online) The energy splitting as a function of the space distance of two vortices. The inset shows the particle density distributions of two vortices separated by $d = 4$ and $d = 8$.

III. MID-GAP STATES

In last section, we have reviewed that the $p_x + ip_y$ topological SC supports zero mode around vortices. These vortices with topologically protected zero mode obey non-Abelian statistics. In this section, we focus on the mid-gap states induced by the vortex superlattice after considering the coupling between Majorana fermions on different vortices.

To study the coupling between Majorana fermions on different vortices, we assume that each vortex locally threads into single plaquette. Each vortex can be regarded as the end of a string. This string is the phase branch-cut of the pairing order parameter. Each (spinless) fermion denoting by f acquires a minus sign after moving around the vortex by crossing the phase branch-cut as $f \rightarrow -f$. So the vortex is a really π -flux on a plaquette. This definition provides us an effective method to numerically compute the properties of the quantized vortex in the $p_x + ip_y$ topological SC. The inset of Fig.1 shows two vortices with two approximate zero modes localized in each core.

Because the inter-vortex tunneling effect leads to the energy splitting of the two zero modes, we must take into account this tunneling effect for two quantized vortices nearby. To see the tunneling effect clearer, we performed numerical simulations and the results are shown in Fig.1. Generally, the energy splitting due to inter-vortex tunneling is determined by the overlap of the wave functions of two vortices. One can see that the energy splitting between two nearby vortices (the distance d between two vortices nearby is smaller than

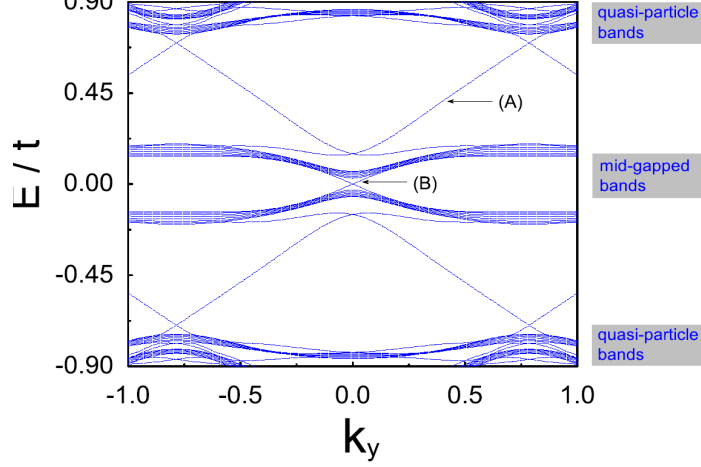


FIG. 2: (Color online) The band structure of the topological superconductor with a vortex superlattice on a cylindrical geometry. (A): the edge state of the parent topological superconductor; (B): the edge state of the mid-gap states induced by the vortex superlattice.

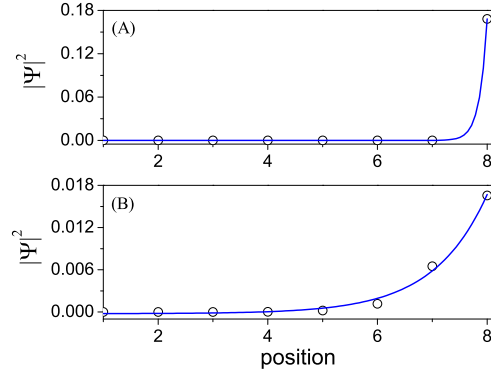


FIG. 3: (Color online) The particle density distribution of the edge states: (A): the edge state of the parent topological superconductor; (B): the edge state of the mid-gap states induced by the vortex superlattice.

the coherent length ξ) exhibits a relatively large value. On the other hand, for two well separated vortices (the distance d between two vortices nearby is larger than the coherent length ξ), the energy splitting from the inter-vortex tunneling can be ignored. In Fig.1, we have chosen $\Delta = -1.0t$ to do our calculations.

A. Mid-gap energy bands and its edge states induced by vortex superlattice

In this part we study the $p_x + ip_y$ topological SC with a square vortex superlattice. The lattice constant of the square vortex superlattice is set to be $d = 4a$. We choose $8a \times 4a$ sites to be a unit cell ($8a$ along x direction and $4a$ along y direction). To show the topological properties of the mid-gap states, we put the system on a cylinder (open boundary condition along x -direction, periodic boundary condition along y -direction). The results are shown in Fig.2. From Fig.2, one can see that the energy bands from the bulk consist of two parts : the energy bands of Bogoliubov quasi-particles and the mid-bands induced by vortex superlattice. Both energy bands have energy gaps. Except for the energy bands from the bulk, there exist gapless edge states. There are two types of edge states: one comes from the parent topological superconductor due to its nontrivial topological properties, the other comes from the vortex superlattice. That means the mid-gap states induced by the vortex superlattice also have nontrivial topological properties. See the illustration in Fig.2 and Fig.3. Fig.3(A) shows the particle density distribution of the edge state of the parent topological superconductor and Fig.3(B) shows the particle density distribution of edge states of the mid-gap states induced by the vortex superlattice. One can see that due to a larger energy gap, the localized length into the bulk of the edges state of the parent topological SC is shorter than that of the edge states of the mid-gap states.

B. Effective tight-binding Majorana lattice model

In the last section, we have shown the induced mid-gap energy bands induced by vortex superlattice. Because each vortex has a residual zero mode and the inter-vortex tunneling effect leads to the energy splitting of the degenerated zero modes, we can use a tight-binding Majorana lattice model to describe the mid-gap states proposed in Ref.[14]. The Hamiltonian of this tight-binding Majorana lattice model can be

$$\begin{aligned}
 H_F = & i \sum_l \sum_{|i-j|=l_x} \frac{t_{l_x}}{2} s_{ij}^{l_x} \gamma_i \gamma_j + i \sum_l \sum_{|i-j|=l_y} \frac{t_{l_y}}{2} s_{ij}^{l_y} \gamma_i \gamma_j \\
 & + i \sum_{|i-j|=\sqrt{2}} \frac{t_{\sqrt{2}}}{2} s_{ij}^{\sqrt{2}} \gamma_i \gamma_j,
 \end{aligned} \tag{10}$$

where γ_i is the operator of Majorana fermion in i_{th} vortex core obeying the self-conjugate condition and the canonical commutate relation $\{\gamma_i, \gamma_j\} = 2\delta_{ij}$. The indices $l = 1, 2$ denote

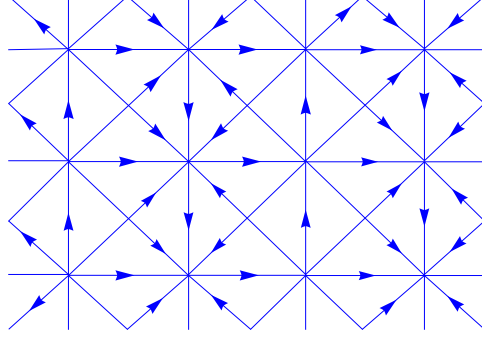


FIG. 4: (Color online) The sketch of the square Majorana lattice. The arrow configuration denotes one possible gauge of the model, $s_{ij} = 1$ if arrow from i to j , the clockwise product of the s_{ij} 's around each triangle is equal to -1 such that each triangular through by $-\pi/2$ flux. And the gauge choice splits the lattice into two sublattices.

nearest neighbor couplings, next-next nearest neighbor couplings, respectively, t_{l_x}, t_{l_y} are the corresponding coupling strength along x and y direction, and $t_{\sqrt{2}}$ is the next nearest neighbor coupling strength. Each s_{ij} connecting bond $\langle ij \rangle$ has Z_2 gauge degree of freedom which does not affect any physical conclusions. Motivated by the decompose rules that two Majorana fermions fuse into a complex fermion, and no net flux through the primitive cell, the condition that there is $-\pi/2$ flux in each triangular plaquette must be satisfied. Fig.4 shows the Majorana lattice model.

We then decompose Majorana operator as

$$\gamma_{2i-1} = f_i + f_i^\dagger, \quad i\gamma_{2i} = f_i - f_i^\dagger, \quad (11)$$

where f_i destroys a Dirac fermion on the center of link (see Fig.4). This formalism reproduces an effective spinless SC state which we model as

$$H_F = \sum_{\mathbf{k}} \begin{pmatrix} f_{\mathbf{k}}^\dagger & f_{-\mathbf{k}} \end{pmatrix} \begin{pmatrix} \phi_{\mathbf{k}}^0 + \phi_{\mathbf{k}}^3 & \phi_{\mathbf{k}}^1 - i\phi_{\mathbf{k}}^2 \\ \phi_{\mathbf{k}}^1 + i\phi_{\mathbf{k}}^2 & \phi_{\mathbf{k}}^0 - \phi_{\mathbf{k}}^3 \end{pmatrix} \begin{pmatrix} f_{\mathbf{k}} \\ f_{-\mathbf{k}}^\dagger \end{pmatrix}. \quad (12)$$

The energy dispersion has the form as

$$E_k = \phi_{\mathbf{k}}^0 \pm |\vec{\phi}_{\mathbf{k}}|,$$

TABLE I: The hopping parameters of the effective Majorana lattice model by fitting from the mid-gap energy bands induced by vortex superlattice (All the parameters given under the fixed chemical potential $u = -2.0$).

	$\Delta = 0.4$	$\Delta = 0.6$	$\Delta = 0.8$	$\Delta = 1.0$	$\Delta = 1.2$	$\Delta = 1.4$
t_{1x}	0.02621	0.01547	0.00741	0.01615	0.03376	0.05682
t_{1y}	0.05872	0.04294	0.03397	0.02984	0.03904	0.05852
$t_{\sqrt{2}}$	0.00897	0.00080	0.00189	0.00325	0.01360	0.02677
t_{2x}	0.00012	-0.0032	-0.00126	0.00009	0.00168	0.00108
t_{2y}	0.0	0.0	0.0	0.0	0.0	0.0
fitness	98.72%	99.80%	99.98%	99.99%	99.83%	95.28%

with $\vec{\phi}_{\mathbf{k}} \equiv (\phi_{\mathbf{k}}^1, \phi_{\mathbf{k}}^2, \phi_{\mathbf{k}}^3)$. The vector $\phi_{\mathbf{k}}^i$ is expressed as

$$\begin{aligned}
\phi_{\mathbf{k}}^0 &= -4t_{2y} \sin 2A\mathbf{k}_y, \\
\phi_{\mathbf{k}}^1 &= 4t_{2x} \sin 2A\mathbf{k}_y - 4t_{1y} \sin A\mathbf{k}_y, \\
\phi_{\mathbf{k}}^2 &= -2t_{1x} \sin 2A\mathbf{k}_x - 4t_{\sqrt{2}} \sin 2A\mathbf{k}_x \cos \mathbf{k}_y, \\
\phi_{\mathbf{k}}^3 &= -2t_{1x} \sin 2A\mathbf{k}_x - 4t_{\sqrt{2}} \cos A\mathbf{k}_y + 2t_{1x} \\
&\quad - 4t_{\sqrt{2}} \cos A\mathbf{k}_y \cos 2A\mathbf{k}_x.
\end{aligned} \tag{13}$$

The calculation for these functions is straightforward (though a little tedious), and the parameter $A = 4$ arises from the vortex-distance $d = 4$.

Next, we obtain the tunneling parameters by fitting the energy dispersion of the mid-gap states induced by the vortex superlattice. As shown in top panel of Fig.5, the energy dispersion of the mid-gap states are obtained by the numerical calculations. The bottom panel shows the energy dispersion of the effective tight-binding Majorana lattice model and the corresponding hopping parameters are given in TABLE.1. We point out that the effective tight-binding Majorana lattice model may describe the mid-gap states very well. So we have an effective method to calculate the quantum properties of the $p_x + ip_y$ SC with vortex superlattice quantitatively, and which can be compared with the experimental research.

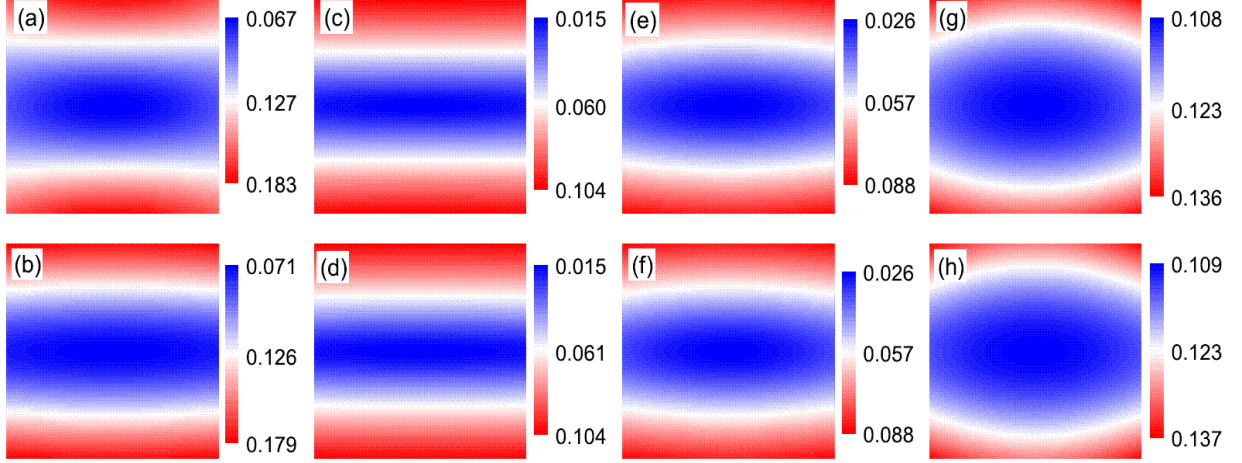


FIG. 5: Top panel: The contour plot of dispersion of mid-gap energy bands induced by vortex superlattice as a function of paired order parameter Δ in the zone $k_x \otimes k_y \in [-0.1, 0.1] \otimes [-0.2, 0.2]$. The paired order parameter is equal 0.4, 0.8, 1.2, and 1.4 for (a), (c), (e), (g), respectively. Bottom panel: The fitting dispersion of the effective tight-binding Majorana lattice model, and the hopping parameters are obtained in TABLE I.

TABLE II: The hopping parameters directly from the energy splitting in Fig.1

	$\Delta = 0.4$	$\Delta = 0.6$	$\Delta = 0.8$	$\Delta = 1.0$	$\Delta = 1.2$	$\Delta = 1.4$
t_{1x}	0.03678	0.03646	0.05522	0.10012	0.16906	0.25598
t_{1y}	0.03679	0.03647	0.05522	0.10017	0.16907	0.25598
$t_{\sqrt{2}}$	0.00120	0.02362	0.02596	0.02533	0.03763	0.07586
t_{2x}	0.00854	0.00394	0.00593	0.01573	0.04501	0.09284
t_{2y}	0.00854	0.00394	0.00593	0.01573	0.04501	0.09284

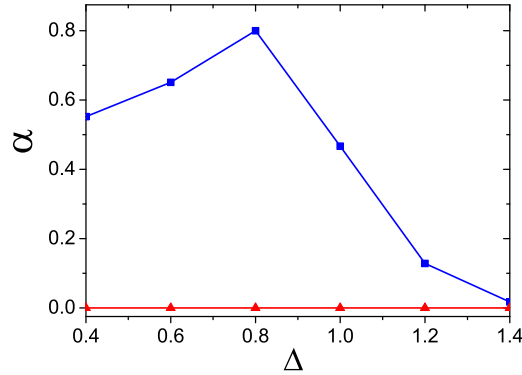


FIG. 6: (Color online) The anisotropic ratio of the effective Majorana lattice model.

C. Anisotropy

An interesting feature of the mid-gap states is the *anisotropy* for the hopping parameters along x-direction and those along y-direction. We define the anisotropic ratio of the effective Majorana lattice model as

$$\alpha = \left| \frac{t_{1y}}{t_{1x}} - 1 \right|. \quad (14)$$

For the case of $\Delta = 0.8t$, the Majorana lattice model is highly anisotropic due to a large anisotropic ratio up to $\alpha \simeq 3.584$. For the case of $\Delta = 1.4t$, the anisotropic ratio is smaller which is about 0.06. The physical mechanism of the enlarged anisotropic ratio is not well understand right now and will be explored in the future.

On the other hand, we can also write down an effective tight-binding Majorana lattice model by calculating the tunneling parameters from the energy splitting given in Fig.1. The results are given in TABLE.2. One can see that the effective tight-binding Majorana lattice model from the energy splitting is almost isotropic, or $\alpha \rightarrow 0$. In particular, from Fig.6, one can see that the tight-binding Majorana lattice model from the energy splitting always fails to describe the mid-gap states.

D. Topological invariant

Another feature of the mid-gap states is the *topology*. We calculate the topological invariant of the effective tight-binding Majorana lattice model. The effective tight-binding

Majorana lattice model is described by the Hamiltonian,

$$H_F = \phi_{\mathbf{k}}^0 \mathcal{I}_{2 \times 2} + \sum_i \sigma_i \phi_{\mathbf{k}}^i.$$

Thus, the topological invariant of the model is the winding number [13, 15]

$$\mathcal{C} = \int_{\mathbf{k} \in \text{BZ}} \frac{d^2 \mathbf{k}}{4\pi} \vec{\phi} \cdot \partial_{\mathbf{k}_x} \vec{\phi} \times \partial_{\mathbf{k}_y} \vec{\phi}, \quad (15)$$

The winding number classifies different homotopy classes mapping from 2D BZ to 2D sphere, $\phi_n(\mathbf{k}) : T^2 \rightarrow S^2$. Note that the winding number also associates with the Hamiltonian $\mathcal{H}_0 = \sum_i \sigma_i \phi_{\mathbf{k}}^i$. And these two Hamiltonians are topologically equivalent by a adiabatic deformation connecting H_F and \mathcal{H}_0 without closed the bulk gap. We perform the integral Eq.(15) in irreducible Brillouin zone $\mathbf{k}_x \otimes \mathbf{k}_y \in [-\pi/8, \pi/8] \otimes [-\pi/4, \pi/4]$, which gives the value $\mathcal{C} = 1$ (first column data). So the effective tight-binding Majorana lattice model is just a "topological SC state" within our construction formalism. Such hierarchical effect had been employed to understand the topological quantum transition induced by vortex excitation that has been studied in the context of Kitaev's honeycomb model supporting non-Abelian anyon excitation[14, 16, 17].

IV. CONCLUSION

In conclusion, we have studied the $p_x + ip_y$ topological SC with a square vortex superlattice. Due to the inter-vortex tunneling, there exist mid-gap energy bands induced by the vortex superlattice. We found that such mid-gap energy bands have nontrivial topological properties including the gapless edge states and non-zero winding number. Then we write down an effective anisotropic tight-binding Majorana lattice model to characterize the mid-gap states and obtain the hopping parameters by fitting the energy dispersion with numerical calculations. In particular, we find that the anisotropic tight-binding Majorana lattice model has nontrivial topological properties.

* * *

This work is supported by National Basic Research Program of China (973 Program) under the grant No. 2011CB921803, 2012CB921704 and NSFC Grant No. 11174035.

V. APPENDIX: THE DERIVATION OF BDG EQUATION

In this appendix, we give the derivation of BdG equation corresponding to Eq.(6). The starting point is a general BCS mean field Hamiltonian

$$H_{BCS} = \int d\mathbf{r} \psi^\dagger(\mathbf{r}) \left(-\frac{\partial^2}{2m} - u \right) \psi(\mathbf{r}) + \frac{1}{2} \int \int d\mathbf{r} d\mathbf{r}' \{ \psi^\dagger(\mathbf{r}) \Delta(\mathbf{r}, \mathbf{r}') \psi^\dagger(\mathbf{r}') + h.c. \}, \quad (16)$$

where the pairing function $\Delta(\mathbf{r}, \mathbf{r}')$ is given by

$$\Delta(\mathbf{r}, \mathbf{r}') = \Delta\left(\frac{\mathbf{r} + \mathbf{r}'}{2}\right) (\partial_{x'} + i\partial_{y'}) \delta(\mathbf{r} - \mathbf{r}'). \quad (17)$$

To diagonalize this Hamiltonian, it's useful to perform the Bogoliubov transformation

$$\psi(\mathbf{r}) = \sum_n [\gamma_n u_n(\mathbf{r}) + \gamma_n^\dagger v_n^*(\mathbf{r})], \quad (18)$$

where index n labels n_{th} quasi-particle eigenstates. The complex functions $u_n(\mathbf{r})$ and $v_n(\mathbf{r})$ are determined by the following requirement

$$[H_{BCS}, \gamma_n] = -E_n \gamma_n. \quad (19)$$

The commutators of the field operator and the Hamiltonian is easily calculated, which generate

$$[H_{BCS}, \psi(\mathbf{r})] = -\left(-\frac{\partial^2}{2m} - u\right) \psi(\mathbf{r}) - \frac{1}{2} [\Delta(\mathbf{r}) (\partial_x + i\partial_y) + (\partial_x + i\partial_y) \Delta(\mathbf{r})] \psi^\dagger(\mathbf{r}). \quad (20)$$

Substituting the Bogoliubov transformation $\psi(\mathbf{r}) = \sum_n [\gamma_n u_n(\mathbf{r}) + \gamma_n^\dagger v_n^*(\mathbf{r})]$ into the commutator and considering the diagonalization condition yield

$$\begin{aligned} [H_{BCS}, \psi(\mathbf{r})] &= -E_n u_n(\mathbf{r}) \gamma_n - E_n v_n^*(\mathbf{r}) \gamma_n^\dagger \\ &= -\left(-\frac{\partial^2}{2m} - u\right) [\gamma_n u_n(\mathbf{r}) + \gamma_n^\dagger v_n^*(\mathbf{r})] \\ &= -\frac{1}{2} \{ \Delta(\mathbf{r}), \partial_x + i\partial_y \} [\gamma_n u_n(\mathbf{r}) + \gamma_n^\dagger v_n^*(\mathbf{r})]. \end{aligned} \quad (21)$$

Then the coefficients of operator γ_n give

$$\left(-\frac{\partial^2}{2m} - u\right) u(\mathbf{r}) + \frac{1}{2} \{ \Delta(\mathbf{r}), \partial_x + i\partial_y \} v(\mathbf{r}) = E u(\mathbf{r}). \quad (22)$$

And the coefficients of operator γ_n^\dagger give (after performing a conjugation)

$$\left(\frac{\partial^2}{2m} + u\right)v(\mathbf{r}) - \frac{1}{2}\{\Delta^*(\mathbf{r}), \partial_x - i\partial_y\}v(\mathbf{r}) = Ev(\mathbf{r}). \quad (23)$$

These two equations are just the BdG equation

$$H_{BdG}(u(\mathbf{r}), v(\mathbf{r}))^T = E(u(\mathbf{r}), v(\mathbf{r}))^T \quad (24)$$

where

$$H_{BdG} = \begin{pmatrix} -\frac{\partial^2}{2m} - u & \frac{1}{2}\{\Delta(\mathbf{r}), \partial_x + i\partial_y\} \\ -\frac{1}{2}\{\Delta^*(\mathbf{r}), \partial_x - i\partial_y\} & \frac{\partial^2}{2m} + u \end{pmatrix}. \quad (25)$$

It's sufficient to ignore the kinetic term $\frac{-\partial^2}{2m}$, and only consider the one-body part by a varying function $-u(\mathbf{r})$ for studying the topological properties. It is valid by supposing that the energy gap is never closed [6].

-
- [1] X. G. Wen, Int. J. Mod. Phys. B **4**, 239 (1990).
 - [2] X. G. Wen, Adv. Phys. **44**, 405 (1995).
 - [3] D. J. Thouless, M. Kohmoto, M. P. Nightingale, and M. den Nijs, Phys. Rev. Lett. **49**, 405 (1982).
 - [4] C. L. Kane and E. J. Mele, Phys. Rev. Lett. **95**, 226801 (2005).
 - [5] B. A. Bernevig and S. C. Zhang, Phys. Rev. Lett. **96**, 106802 (2006).
 - [6] N. Read and D. Green, Phys. Rev. **B 61**, 10267 (2000).
 - [7] Ady Stern, Nature, **464** (2010).
 - [8] A. Kitaev, Ann. Phys. **321**, 2 (2006).
 - [9] M. Freedman, M. Larsen, and Z. Wang, Math. Phys. **227**, 605 (2002).
 - [10] L. S. Georgiev, Phys. Rev. **B 74**, 235112 (2006). L. S. Georgiev, Nucl. Phys. **B 789**, 552-590 (2008).
 - [11] C. Nayak, S. H. Simon, A. Stern, M. Freedman, and S. Das Sarma, Rev. Mod. Phys. **80**, 1083 (2008).
 - [12] J. Alicea, Rep. Prog. Phys. **75**, 076501 (2012).
 - [13] M. Cheng, R. M. Lutchyn, V. Galitski, and S. Das Sarma, Phys. Rev. Lett **103**, 107001 (2009).
M. Cheng, R. M. Lutchyn, V. Galitski, and S. Das Sarma, Phys. Rev. B **82**, 094504 (2010).

- [14] J. Zhou, Y. J. Wu, R. L. Wu, S. P. Kou, EPL, **102** 47005 (2013).
- [15] X. L. Qi, Y. S. Wu, and S. C. Zhang, Phys. Rev. B **74**, 045125 (2006).
- [16] V. Lahtinen, A. W. W.Ludwig, J. K. Pachos, and S. Trebst, Phys. Rev. B **86**, 075115 (2012).
- [17] V. Lahtinen, New. J. Phys. **13**, 075009 (2011).